Live Cell Imaging of In Vitro Human Trophoblast Syncytialization

Author(s): Rui Wang, Yan-Li Dang, Ru Zheng, Yue Li, Weiwei Li, Xiaoyin Lu, Li-Juan Wang, Cheng Zhu, Hai-Yan Lin, and Hongmei Wang
Source: Biology of Reproduction, 90(6) 2014.
Published By: Society for the Study of Reproduction
URL: http://www.bioone.org/doi/full/10.1095/biolreprod.113.114892

BIOLOGY OF REPRODUCTION (2014) **90**(6):117, 1–10
Published online before print 16 April 2014.
DOI 10.1095/biolreprod.113.114892

Live Cell Imaging of In Vitro Human Trophoblast Syncytialization[1]

Rui Wang,[4,5,6] Yan-Li Dang,[4,7] Ru Zheng,[5,6] Yue Li,[5] Weiwei Li,[5,8] Xiaoyin Lu,[5,6] Li-Juan Wang,[5] Cheng Zhu,[5] Hai-Yan Lin,[3,5] and Hongmei Wang[2,5]

[5]*State Key Laboratory of Reproductive Biology, Institute of Zoology, Chinese Academy of Sciences, Beijing, China*
[6]*Graduate School of Chinese Academy of Sciences, Beijing, China*
[7]*Department of Obstetrics and Gynecology, the 306th Hospital of PLA, Beijing, China*
[8]*College of Life Science, Beijing Normal University, Beijing, China*

ABSTRACT

Human trophoblast syncytialization, a process of cell-cell fusion, is one of the most important yet least understood events during placental development. Investigating the fusion process in a placenta in vivo is very challenging given the complexity of this process. Application of primary cultured cytotrophoblast cells isolated from term placentas and BeWo cells derived from human choriocarcinoma formulates a biphasic strategy to achieve the mechanism of trophoblast cell fusion, as the former can spontaneously fuse to form the multinucleated syncytium and the latter is capable of fusing under the treatment of forskolin (FSK). Live-cell imaging is a powerful tool that is widely used to investigate many physiological or pathological processes in various animal models or humans; however, to our knowledge, the mechanism of trophoblast cell fusion has not been reported using a live- cell imaging manner. In this study, a live-cell imaging system was used to delineate the fusion process of primary term cytotrophoblast cells and BeWo cells. By using live staining with Hoechst 33342 or cytoplasmic dyes or by stably transfecting enhanced green fluorescent protein (EGFP) and DsRed2-Nuc reporter plasmids, we observed finger-like protrusions on the cell membranes of fusion partners before fusion and the exchange of cytoplasmic contents during fusion. In summary, this study provides the first video recording of the process of trophoblast syncytialization. Furthermore, the various live-cell imaging systems used in this study will help to yield molecular insights into the syncytialization process during placental development.

BeWo, developmental biology, live imaging, placental development, placentation, pregnancy, primary cultured cytotrophoblast cells, syncytialization, syncytiotrophoblast, trophoblast

INTRODUCTION

During embryo implantation and placentation, the placental trophoblast plays an important role in fetal–maternal communication. Human placental villous cytotrophoblast cells (CTBs) differentiate by (1) undergoing an epithelial-mesenchymal transition-like change and forming highly invasive extravillous trophoblast cells to anchor the placenta into the maternal uterus and establish fetal–maternal circulation, or 2) fusing and forming the multinucleated syncytium via a process termed syncytialization [1, 2]. The syncytiotrophoblast (STB), the multinucleated syncytium forming the outer layer of the placental villi, is involved in establishing the natural barrier between the mother and developing fetus, which exchanges gas, ingests nutrition, and eliminates waste [3]. Well-formed syncytiotrophoblast in a placenta is very important to a successful pregnancy. Inadequate formation of this structure may lead to severe pregnancy disorders such as pre-eclampsia [4].

The very first method, and one of the most important, used to study syncytialization is electron microscopy, by which placental ultrastructures have been examined and illustrated. First, many differences can be found among placentas from various stages of a human pregnancy. For example, more Hofbauer and Langhans cells and more cells of a transitional form between the cytotrophoblast and syncytiotrophoblast can be found in the first trimester placenta than in the term placenta [5–7]. Next, numerous variations in cellular organelles between the mononucleated cytotrophoblast layer and the multinucleated syncytiotrophoblast have been described. For example, a layer of dynamic microvilli can be found on the surface of the syncytiotrophoblast [8]. Furthermore, a form of a blunt pseudopodial cytoplasmic structure projects from CTBs into the syncytiotrophoblast and is characterized by a double membrane and dilations of the endoplasmic reticulum and mitochondria [9].

Morphologically, CTBs fuse continuously with the overlying syncytiotrophoblast to maintain a functional syncytiotrophoblast layer throughout pregnancy [10]. Therefore, the syncytiotrophoblast is constantly supplied with fresh components from the fusing cytotrophoblasts. Not only cytoplasm but also CTB nuclei are deposited into the multinucleated layer. In 1968, a hormone-synthesizing human choriocarcinoma cell line, BeWo, was established [11], which has been widely used as a model for mimicking trophoblast cell fusion in vitro under forskolin (FSK) treatment [12]. In 1986, primary CTBs isolated from human term placentas were found to be capable of differentiating and fusing spontaneously to form functional syncytiotrophoblast [13]. In 2006, a floating first-trimester villous explant model, called a syncytiotrophoblast denudation and regeneration model, was developed in which the syncytium-denuded villi could spontaneously reform the syncytiotrophoblast layer after 48 h of culture [14]. The above-mentioned models have been utilized to clarify key molecules involved in trophoblast syncytialization.

[1]Supported by National Key Basic Research Program of China grant 2011CB944400 and Natural Science Foundation of China grants 81225004 and 81322008.
[2]Correspondence: Hongmei Wang, Institute of Zoology, Chinese Academy of Sciences, 1 Beichen West Road, Chaoyang District, Beijing 100101, China. E-mail: wanghm@ioz.ac.cn
[3]Correspondence: Hai-Yan Lin, Institute of Zoology, Chinese Academy of Sciences, 1 Beichen West Road, Chaoyang District, Beijing 100101, China. E-mail: linhy@ioz.ac.cn
[4]These authors contributed equally to this work.

Received: 14 October 2013.
First decision: 9 November 2013.
Accepted: 28 March 2014.

eISSN: 1529-7268 http://www.biolreprod.org
ISSN: 0006-3363

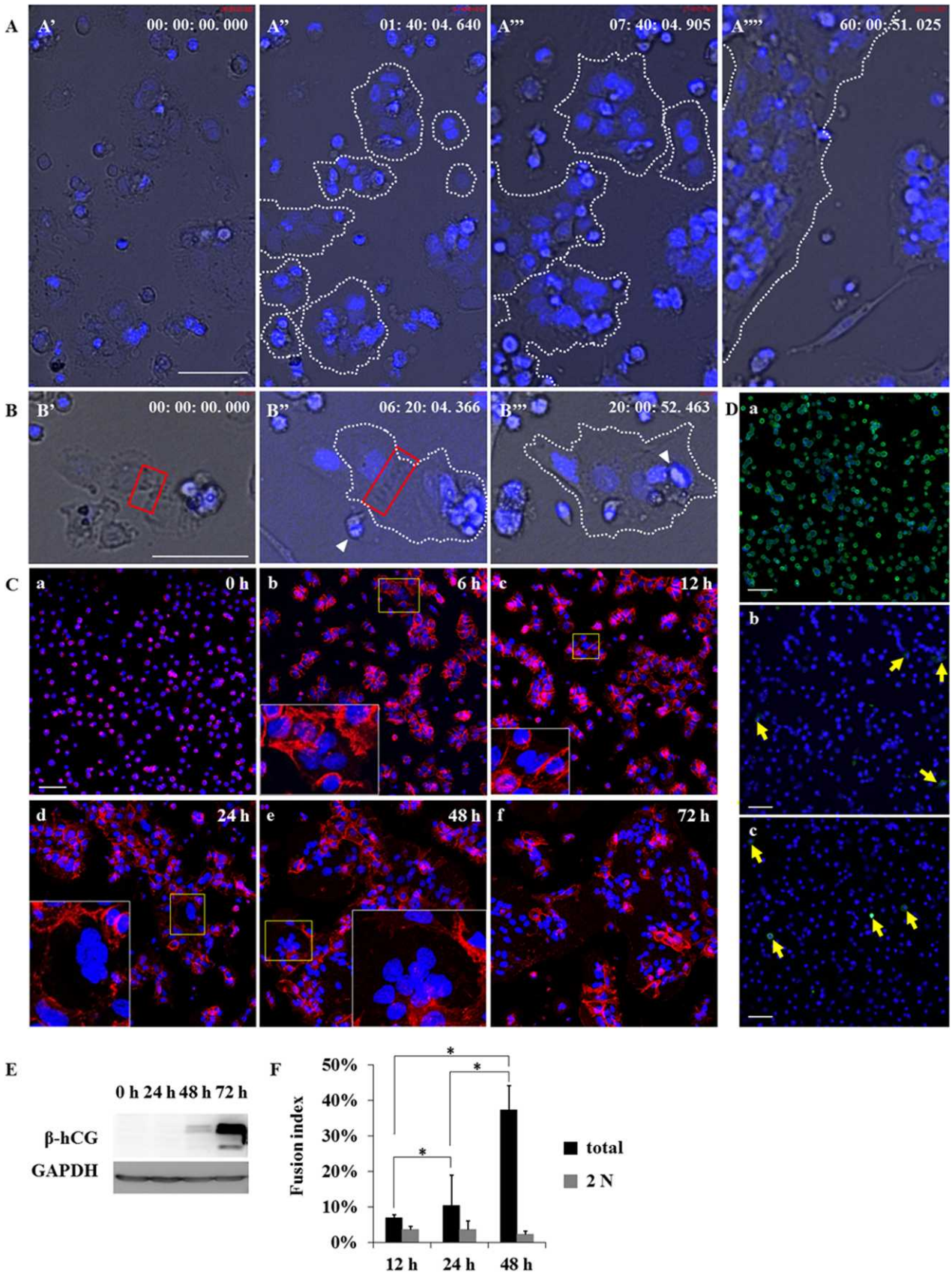

FIG. 1. Live cell imaging of the spontaneous syncytialization of primary cultured human term cytotrophoblast cells (CTBs). **A**) Primary CTBs isolated from a term placenta (**A**′) were stained with Hoechst 33342 dye. Still images from Supplemental Movies S1 (**A**) and S2 (**B**) are shown. Small cell clusters formed first (**A**″) and sequentially aggregated with each other (**A**‴) until a large aggregate/syncytium-like structure was formed (**A**‴). **B**) A large aggregate/syncytium-like structure was formed from several mononucleated cells. **B**′) At first, two cells approached each other (red box). **B**″) Next, some finger-like protrusions from each cell began to contact each other (red box). **B**‴) Finally, a syncytium-like structure was formed (area inside dotted line). The white arrowhead indicates a dead cell. **C**) Membranes of primary CTBs were immunostained with E-cadherin (red), and nuclei were stained with DAPI (blue) to

Apart from placental development, cell fusion is also a developmental program and is an essential process in many other systems and events, including fertilization, fusion in leech [15] and *Chlamydomonas* gametes [16], hyphal fusion in filamentous fungi [17], hypodermal cell fusions in the *Caenorhabditis elegans* hermaphrodite [18], myoblast fusion [19], and the formation of osteoclasts from monocytes [20–23]. Using live-cell imaging combined with other strategies, many interesting structures or molecules related to cell-cell fusion have been elucidated. For example, the fusion pore in the *C. elegans* epidermis [24] and the invasive podosome-like structure in myogenesis of the *Drosophila* embryo [25] have been described, and the F-family fusogens in *C. elegans*, epithelial fusion failure 1 (EFF-1) [26–28], and anchor cell fusion failure 1 (AFF-1) [29] have been discovered.

However, to date, no live-cell imaging report has recorded the process of trophoblast syncytium formation. Deciphering the nature of syncytialization depends on a complete understanding of the spatial and temporal process of trophoblast cell-cell fusion and its respective biochemical machinery. In this study we traced the fusion process in primary cultured CTBs and BeWo cells by using a live-cell imaging system. Using different color systems, including live staining with Hoechst 33342 or cytoplasmic CellTracker (Invitrogen) dyes [30], and stably expressing enhanced green fluorescent protein (EGFP) or DsRed2-Nuc in BeWo cells, we observed finger-like protrusions on the membranes of neighbor fusion partners and cytoplasmic exchange between cells during fusion. These different live-cell imaging systems first established in the present study will help to further our understanding of the process of trophoblast fusion and its underlying mechanisms.

MATERIALS AND METHODS

Tissue Collection

Human placental tissues were collected in accordance with the policy of the Ethics Committee of the 306th Hospital of the People's Liberation Army. Informed consent was obtained from all women who donated their placentas. Samples were used according to standard experimental protocols approved by the Ethics Committee of the Institute of Zoology, Chinese Academy of Sciences. For the spontaneous syncytialization studies, three term placentas delivered by cesarean section were collected under sterile conditions.

Cell Culture and Fusion Assay

Isolation of CTBs from human term placentas was performed as previously described [31]. Briefly, the placenta was cut into pieces and digested in Dulbecco modified Eagle medium (DMEM) with 0.125% trypsin and 0.03% DNase-I (Sigma). CTBs were separated by using Percoll method (GE Healthcare Bio-sciences AB) density gradient centrifugation. Trophoblast cells in the harvested cells were indicated by positive staining of cytokeratin 7 (CK7), a marker for trophoblast cells. Contamination of syncytial fragments was determined by staining for β-subunit of human chorionic gonadotropin (β-hCG) [13] or placental alkaline phosphatase (PLAP) [32]. Cells (2×10^6 cells) were plated in 35-mm dishes in Iscove modified eagle medium (IMEM) with 10% FBS, 100 U/ml penicillin and 100 μg/ml streptomycin and cultured in a 5% CO_2/95% air incubator at 37°C. CTBs that spontaneously fused to form syncytia in vitro were confirmed by E-cadherin immunostaining and Western blot analysis of β-hCG.

The human choriocarcinoma cell line BeWo was obtained from American Type Culture Collection. BeWo cells were maintained in Ham F-12K (Kaighn) medium (Gibco BRL)/ DMEM (1:1 dilution; Hyclone) containing 10% fetal bovine serum (FBS; Gibco BRL), 100 U/ml penicillin, and 100 μg/ml streptomycin in 5% CO_2/95% air at 37°C. BeWo cells were treated with 50 μM FSK (Sigma-Aldrich) for 48 h, and cell fusion was assessed by (1) immunofluorescence using an anti-human E-cadherin antibody to show the cell membrane, followed by staining the nuclei with DAPI; or by (2) Western blotting of the whole-cell lysates using an anti-β-hCG antibody.

The total fusion index was determined by $(N - S)/T$, where N is the number of nuclei in the syncytia, S is the number of syncytia, and T is the total number of nuclei [33]. The two-cell fusion index was calculated as a percentage of double-nucleated cells/total nuclei. For CellTracker staining, the syncytium was designated the cell with a double-fluorescent cytoplasm [30]. All experiments were performed in triplicate. Cells in five randomly selected nonoverlapping fields were counted using microscopy. On average, there were approximately 350 cells in every selected field for the CTBs and 100 cells for the BeWo cells. Results are presented as means ± SEM. Statistical analysis was performed by one-way ANOVA and paired-sample *t*-test, which was performed by using Statistical Package for Social Science software (SPSS for Windows [Microsoft] version 10.0; SPSS Inc.). P values <0.05 were considered significant.

Immunofluorescence

Cells were fixed in 4% paraformaldehyde or ice-cold methanol. Staining of CK7 (product no. ab20206; Abcam) and E-cadherin (product no. sc-71008; Santa Cruz Biotechnology) was performed as previously described [2]. For β-hCG (1:200 dilution; product Z2108; Zeta Corp) and PLAP (1:200 dilution; product sc-47691; Santa Cruz Biotechnology) staining, cells were fixed with ice-cold methanol and incubated at 4°C overnight. Cells were washed with phosphate-buffered saline with Tween 20 (PBST) and incubated with the appropriate highly cross-adsorbed Alexa Fluor 488 goat anti-mouse immunoglobulin G (IgG; product A-21424; Molecular Probes) or Alexa Fluor 555 goat anti-mouse IgG (product A-11029; Molecular Probes). Images were acquired using confocal laser-scanning microscopy with a 20× or 63× objective lens (model LSM 780; Carl Zeiss), and image analysis (LSM Image Browser software; Zeiss). Antibody specificity was confirmed by incubating the slides with normal serum from the same species in which the primary antibody was generated.

Western Blotting

Whole-cell proteins were extracted with SDS lysis buffer (2% SDS, 50 mM Tris-HCI, pH 7.6, 2 mM EDTA, and 10% glycerol). Proteins were quantified using the BCA protein assay kit (Pierce Biotechnology). Twenty micrograms of extracted total proteins was subjected to SDS-PAGE and transferred electrophoretically onto pure nitrocellulose blotting membrane (Pall Corp). After blocking with 5% skim milk, the membrane was sequentially incubated with primary antibodies against β-hCG (code ab54410; Abcam) and GAPDH (code ab37187; Abcam) and with horseradish peroxidase-conjugated secondary antibodies. Signals were developed using the Gene Gnome imaging system (Syngene Bio-imaging).

CellTracker Staining

BeWo cells or primary cultured CTBs were separated into two populations and stained with 10 μM CellTracker Green CMFDA (5-chloromethylfluorescein diacetate; Molecular Probes, Invitrogen) or 10 μM CellTracker Orange CMRA (Molecular Probes, Invitrogen) for 30 min at 37°C in the dark. Cells were then centrifuged for 5 min to replace the staining solution and were resuspended with fresh, pre-warmed medium containing 10% FBS. After incubating in the cell incubator for 30 min, the cells were washed three times with medium containing 10% FBS. Finally, the two populations were diluted to 1×10^6/ml, mixed (5×10^5/ml green-colored cells and 5×10^5/ml red-colored cells per 1 ml of culture medium) and plated in 35-mm dishes for live-cell imaging and Western blotting.

show multinucleated syncytia (insets show higher magnification [3× zoom]) and mononucleated cells at different time points ([**a**] 0 h; [**b**] 6 h; [**c**] 12 h; [**d**] 24 h; [**e**] 48 h; [**f**] 72 h) during spontaneous fusion. **D**) Primary CTBs used for live-cell imaging were simultaneously separated for immunofluorescence staining of CK7 ([**a**] green), β-hCG ([**b**] green, marked by arrows) and PLAP ([**c**] green, marked by arrows). Blue, DAPI. **E**) A representative Western blot shows an increase in β-hCG expression during spontaneous fusion. All experiments were repeated in triplicate, and representative results are shown. **F**) The total fusion index and 2-cell fusion index were determined over a 2-day time course at 12, 24, and 48 h during the spontaneous fusion of primary human term cytotrophoblast cells (*$P < 0.05$). Bars = 50 μm.

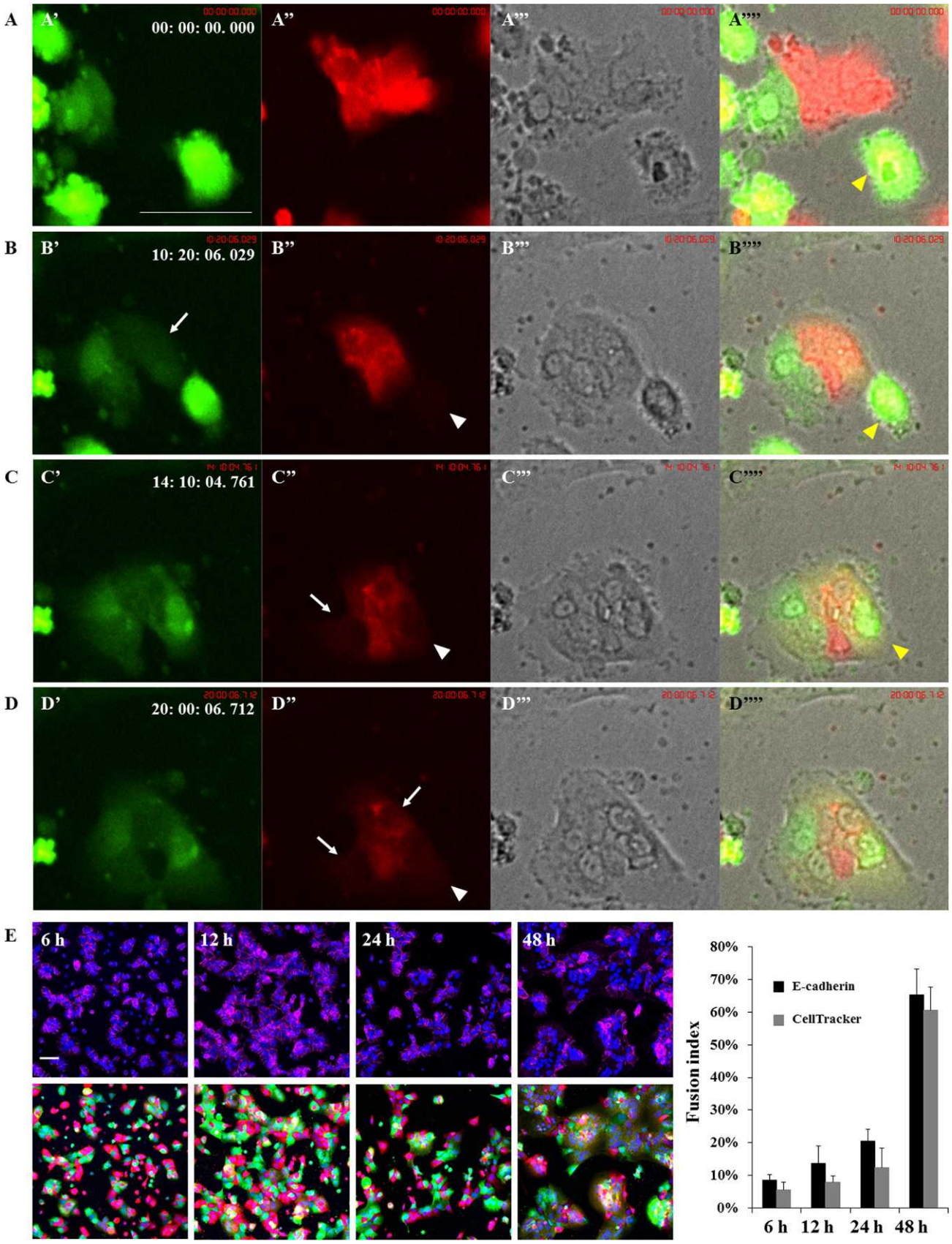

FIG. 2. Live cell imaging of the spontaneous syncytialization of primary human CTBs using cytoplasmic CellTracker dyes. **A–D**) Primary CTBs were separately stained with CellTracker Green CMFDA or CellTracker Orange CMRA and mixed together for further culture. Still images from Supplemental Movie S3. At the beginning, the green mononucleated cell on the left and the red multinucleated cell on the right remained next to each other (**A**′ and **A**‴). During the fusion process, green signals flowed into the red cell ([**B**′] white arrow), and then the red signal appeared in the green cell ([**C**″] white arrow). When the syncytium was formed, a homogeneous color could be observed (**D**). The green fluorescence of the third neighbor cell diffused after fusing with

Establishment of EGFP- or DsRed2-Nuc-Overexpressing BeWo Cell Line

BeWo cells were transfected with pEGFP-N1 or pDsRed2-Nuc reporter plasmids (Clontech Laboratories Inc.) by using the Neon transfection system (Invitrogen) according to the manufacturer's instruction. Briefly, 5×10^5 cells were resuspended in resuspension buffer (Invitrogen) at a density of 1×10^7 cells/ml and incubated with 5 μg of plasmid. The transfection was performed at room temperature using Program 17 (850 volts, 30 ms, 2 pulses). Subsequently, cells were seeded into a 24-well cell culture plate. Two days after transfection, the cells were subjected to antibiotic selection using 1 mg/ml neomycin in 35-mm-diameter cell culture dishes in a humidified 37°C/5% CO_2 incubator, and the neomycin-resistant clones were expanded for further studies.

Live-Cell Imaging

For primary cultured CTBs, cells were plated in 35-mm tissue culture-treated culture dishes (Corning) 12 h prior to video microscopy. For BeWo cells, cells were plated in 8-well chamber slides (Nunc; Thermo Fisher Scientific) in culture medium containing 10% FBS, 100 U/ml penicillin, and 100 mg/ml streptomycin and subjected to FSK (50 μM) treatment after attachment. Cells were imaged using an Eclipse Ti model inverted microscope with a 20×objective lens (numerical aperture, 0.95; Nikon), an Orca ER model camera (Hamamatsu), and a Perfect Focus System. The microscope was surrounded by a custom-made enclosure to maintain constant temperature (37°C) and atmosphere (5% CO2 and 95% air). The filter sets used were as follows: Hoechst 33342, 405 nm (excitation); green fluorescent protein (GFP), 488 nm (excitation); and RFP, 561 nm (excitation). Laser power was maintained at less than 10%. For BeWo cells and CellTracker-stained primary cells, we acquired 6 z sections with a step size of 0.75 μm in Hoechst 33342, GFP, and DsRed2 channels. For primary cells stained only with Hoechst 33342 dye, we did not acquire a z section. Image acquisition was controlled by using Volocity software (Perkin-Elmer). For human primary CTBs, the time-lapse images were recorded every 10–20 min for 48–60 h. For BeWo cells, the time-lapse images were recorded every 10–15 min for 48 h.

RESULTS

Live-Cell Imaging of Spontaneous Syncytialization of Primary Cultured CTBs from a Term Placenta

To dynamically trace the process of trophoblast cell fusion, human primary CTBs were freshly isolated from a term placenta and stained with Hoechst 33342 dye. As shown in Figure 1A and Supplemental Movie S1 (all supplemental data are available online at www.biolreprod.org) mononucleated CTBs migrated to each other and formed a large aggregate/syncytium-like structure with more than 40 nuclei. In detail, at the early stage of the syncytialization process, single mononucleated cells (Fig. 1A′) began to aggregate (Fig. 1A″, area inside dotted line). Then, the cells gathered to form larger cell clusters (Fig. 1A‴, area inside dotted line). Eventually, a large aggregate/syncytium-like structure was established that displayed a uniformly distributed cytoplasm (Fig. 1A‴, area inside dotted line), and this process usually lasted for dozens of hours. After visualization of aggregation and possibly trophoblast fusion, we attempted to trace single cell-cell fusion. After plating, two mononucleated cells migrated vigorously and contacted each other with many protrusions (Fig. 1B′, red rectangular area). Remarkably, some protrusions from the two neighboring cells formed finger-like structures on the cell membranes of the leading edges of the fusion partners (Fig. 1B″, red rectangular area). Disappearance of the finger-like protrusions might indicate a cell-cell fusion, and finally a syncytium-like structure was formed (Fig. 1B‴, Supplemental Movie S2). To substantiate the syncytium formation profiled by live-cell imaging, we simultaneously separated cell populations for immunofluorescence staining with the cell membrane marker E-cadherin. As shown in Figure 1C, there were small syncytia with two or more nuclei (Fig. 1C, b–d), whereas most of the other cells aggregated during the first 24 h of culture. Later, single cells and small syncytia continued to aggregate or fused to form cell clusters (Fig. 1C, e and f) or larger syncytia (Fig. 1C, e and f). More than 95% of the isolated cells were trophoblast cells as indicated by CK7-positive staining (Fig. 1D, a). To verify that most of the cells were cytotrophoblast cells rather than STB fragments, we performed immunofluorescence analysis of β-hCG and PLAP. As shown in Figure 1D, b and c, less than 2% of the cells were positive for these two markers (Fig. 1, yellow arrows). In this respect, most of the isolated cells were relatively pure CTBs with minimal STB fragment contamination. A Western blot assay of β-hCG production showed that β-hCG dramatically increased during the time of spontaneous syncytialization (Fig. 1E). To determine whether the multinucleated cells would allow single cells to fuse or would prevent new single cell-cell fusions from occurring, we performed numerical assessment of the proportion of cells that initially formed a 2-cell fusion in the context of the total fusion indices at 3 time points (12, 24, and 48 h) (Fig. 1F). The results showed that the two-cell fusion indices were approximately 3% at each time point, and no significant differences were found among the three time points.

To better define the multinucleated structure as a syncytium, we separated the primary CTBs into two populations and stained them with CellTracker Green CMFDA or CellTracker Orange CMRA cytoplasmic dyes. The two populations of cells were mixed, and the cells exhibited either a green or red fluorescent cytoplasm by fluorescence microscopy (Fig. 2A). Cell-cell fusion occurred between green cells, red cells or a green, and red cells. Figure 2, A–D, and Supplemental Movie S3 show the fusion process, first, between a green mononucleated cell and a red multinucleated cell and then between another green double-nucleated cell and the newly formed syncytium. First, the cytoplasm of the green cell flowed into the neighboring red fusion partner (Fig. 2B′, white arrow). Next, the red signals flowed into the green cell (Fig. 2C″, white arrow). The newly formed syncytium exhibited a double-fluorescent cytoplasm (Figs. 2C′, C″, and 2C‴, yellow to light orange in the merged image). During fusion of the former two partners, a third green cell (Fig. 2, yellow arrowhead) joined and deposited its green cytoplasm into the orange cytoplasm of the newly formed syncytium (Fig. 2C‴). Meanwhile, the red signals also flowed into the third green cell (Fig. 2, B″ and C″, white arrowhead). Later, the cytoplasm mixed homogeneously (Fig. 2D).

Live-Image Profiling of Syncytium Formation of BeWo Cells after FSK Treatment

Furthermore, we used an FSK-induced fusion model with the choriocarcinoma cell line BeWo. Two populations of cells were stained separately with CellTracker Green CMFDA or Orange CMRA and Hoechst 33342 dye, mixed and treated

the syncytium ([**A**‴, **B**‴, and **C**‴] yellow arrowhead), and red signals appeared in this green cell ([**B**″, **C**″, and **D**″] white arrowhead). **A**‴, **B**‴, **C**‴, and **D**‴) Brightfield views. **A**‴, **B**‴, **C**‴, and **D**‴) Merged images. **E**) The kinetics of trophoblast cell-cell fusion were analyzed over a 2-day course at 6, 12, 24, and 48 h for primary cultured CTBs, using either E-cadherin immunostaining or CellTracker Green/Orange staining. Pink, E-cadherin; green, CellTracker Green; red, CellTracker Orange; blue, DAPI. The color of the red cell stained with CellTracker Orange (approximate fluorescence excitation/emission maxima = 548/576 nm, respectively) is a pseudocolor. Bars = 50 μm.

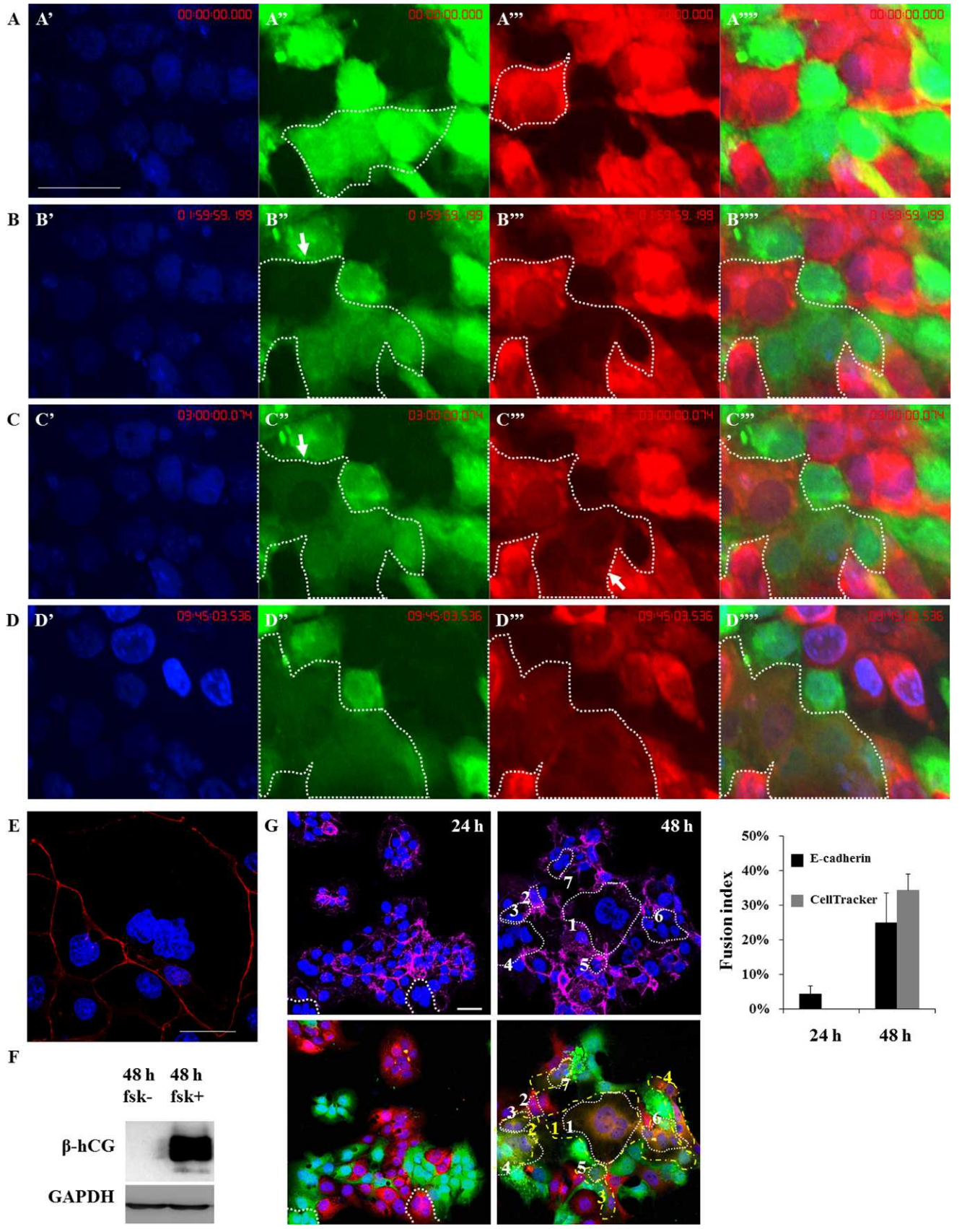

FIG. 3. Visualization of BeWo cell-cell fusion after FSK treatment. **A–D**) BeWo cells were separately stained with CellTracker Green CMFDA or CellTracker Orange CMRA and co-cultured with exposure to FSK for 48 h. Still images from Supplemental Movie S4. Nuclei were stained with Hoechst 33342 dye (**A**′, **B**′, **C**′, and **D**′). (**A**) A green cell ([**A**″] area inside dotted line) was next to a red cell ([**A**‴] area inside dotted line). (**B**) The green cytoplasm flowed gradually into the red cell ([**B**″ and **C**″] white arrows), and the red cytoplasm flowed into the green cell ([**C**‴] white arrow). When the syncytium was formed, the cytoplasm was uniformly mixed ([**D**″ and **D**‴] area inside dotted line). **A**‴, **B**‴, **C**‴, and **D**‴) Merged images. The color of the red cell

with FSK. The stained cells exhibited either a green (Fig. 3A″) or red (Fig. 3A‴) fluorescent cytoplasm under fluorescence microscopy. Meanwhile, all nuclei were visualized by blue fluorescence (Fig. 3, A′, B′, C′, and D′). These cells were observed by live-cell microscopy, and the entire process of fusion was recorded as shown in Supplemental Movie S4. First, the green fluorescent cytoplasm flowed into the red fluorescent cytoplasm (Fig. 3B″, white arrow), and then the red fluorescent cytoplasm flowed into the green fluorescent cytoplasm (Fig. 3C‴, white arrow). Finally, the cytoplasm of the newly formed syncytium mixed homogeneously and was visible with a double-fluorescent cytoplasm (Fig. 3D). The success of the establishment of this fusion model upon 48-h FSK treatment was also simultaneously confirmed by E-cadherin immunofluorescence (Fig. 3E) and β-hCG Western blotting (Fig. 3F).

Furthermore, we used both E-cadherin staining and CellTracker staining and compared the fusion index of primary cultured trophoblast cells (Fig. 2E) and FSK-induced BeWo cells (Fig. 3G). For primary cultured CTBs, the fusion index acquired from E-cadherin staining was slightly higher than that from CellTracker staining at each time point. The latter method could generate three patterns of cell fusion, including green-green cell fusion, red-red cell fusion, and green-red cell fusion (Fig. 2E, lower panel). However, the fusion of cells with the same color was difficult to distinguish, which likely accounts for the lower fusion index than that of the E-cadherin method. For BeWo cells, the fusion index assessed from the E-cadherin group was higher than the CellTracker group at the early stage of fusion (24 h of culture) due to the better ability of E-cadherin to delineate the cell boundaries of a very small number of fused cells, especially the fusion of cells with the same color (Fig. 3G, left panel, area within the white dotted line). However, at 48 h of culture, the fusion index of the E-cadherin group was slightly lower than that of the CellTracker group. As shown in Figure 3G, middle panel, both techniques could omit some multinucleated cells; for example, the red-red cell fusion in the CellTracker group (Fig. 3, within the white dotted line) and the unclear syncytium boundary in the E-cadherin (yellow, no. 4) and CellTracker groups (yellow nos. 1, 2, and 3).

Live-Cell Imaging of Trophoblast Cell Fusion Using Fluorescent EGFP and DsRed2-Nuc

Two BeWo cell lines were stably transfected with pEGFP-N1 or pDsRed2-Nuc reporter plasmids. The former line constitutively expressed EGFP and the latter exhibited nucleus-localized *Discosoma* spp. red fluorescent protein (DsRed2-Nuc). The two cell lines were cocultured, and time-lapse images of the formation of multinucleated syncytia (Fig. 4A) expressing both immunofluorescent proteins were recorded (Supplemental Movie S5). A green cell (Fig. 4B, B′, area inside dotted line) was in close proximity to a DsRed2-labeled double-nucleated cell with an invisible cytoplasm (Fig. 4B, B″, area inside dotted line). During the fusion process, the green fluorescence flowed into the cytoplasm of the syncytium with red nuclei (Fig. 4C, yellow dot-dashed line shows the boundary between the fusing partners that gradually vanished, as shown in Supplemental Movie S5). When the fusion was completed, a syncytium containing both red nuclei and uniformly distributed green cytoplasm was visible (Fig. 4D‴).

DISCUSSION

The syncytialization of human placental trophoblasts plays an important role in maintaining a successful pregnancy. Any imbalance in the syncytialization dynamics may be associated with pregnancy-related diseases such as pre-eclampsia [34, 35], a complication characterized by high blood pressure and proteinuria that affects 3%–5% of pregnant women [36]. Several reports have indicated that the master players in syncytialization, including GCM1 and syncytins, are down-regulated in pre-eclampsia [37, 38]. However, increased trophoblast fusion might also contribute to the onset of pre-eclampsia [39]. Thus, to ensure a healthy pregnancy and to better diagnose and treat pre-eclampsia, efforts to understand the nature of syncytialization and its connection with diseases should be approached from a cell biology viewpoint. Because of the lack of availability of models with which to study syncytialization, the basic characteristics underlying trophoblast cell fusion remain unknown. Using live-cell imaging, we report here for the first time the process of syncytialization in a spontaneous fusion model of primary CTBs and an FSK-induced fusion model of BeWo cells.

We observed that primary trophoblast cells isolated from term placentas exhibited high fusion capacity and that noticeable fusion occurred between primary mononucleated CTBs and small multinucleated syncytia. Interestingly, we found finger-like protrusions propelling along the membrane edges of opposing cells during primary cytotrophoblast fusion. These finger-like protrusions are very similar to blunt pseudopodial structures on CTBs that protrude into the syncytiotrophoblast, as observed in early electron microscopy studies on syncytialization [9]. In the well-studied *Drosophila* myoblast fusion model, an asymmetrical fusogenic synapse consisting of an invasive podosome-like structure in one cell and a thin sheath in the opposing cell was visualized by electron and fluorescence microscopy [19, 25]. The podosome-like structure formed during *Drosophila* myoblast fusion is composed of cell adhesion molecules encircling the F-actin-enriched core and is critical for the formation of a fusion pore [19, 40]. The underlying mechanisms include the degradation of ECM components by protease secretion and the generation of a membrane curvature at the tip of each invasive finger by actin polymerization [41]. During the past decade, fusion pores have been found to emerge at the beginning of fusion and to expand to promote cellular substance exchange in many cell fusion types, including exocytosis [42], myoblast fusion [25], and cell fusion events during *C. elegans* development [24]. Therefore, during primary cytotrophoblast fusion, the finger-like protrusion and subsequent formation of a pore-like structure originating at the cell periphery might imply the disassembly of the neighbor cell membrane and cytoskeleton, which allows adhesive interactions and cytoplasmic communications between the fusion partners. Furthermore, we also observed distinct cytoplasmic flow between the fusion partners, until cytoplasmic continuity was established during both

stained with CellTracker Orange (approximate fluorescence excitation/emission maxima = 548/576 nm, respectively) is a pseudocolor. **E**) BeWo cells used for live-cell imaging (**A–D**) were simultaneously immunostained with E-cadherin, and nuclei were stained with DAPI. **F**) A representative Western blot shows an increase in β-hCG expression during FSK-induced BeWo cell fusion. All experiments were repeated three times, and representative results are shown. **G**) The kinetics of trophoblast cell-cell fusion were analyzed over a 2-day time course at 24 and 48 h for FSK-treated BeWo cells, using either E-cadherin immunostaining or CellTracker Green/Orange staining. White or yellow dotted lines mark the syncytia that are illustrated by E-cadherin or CellTracker staining, respectively. Pink, E-cadherin; green, CellTracker Green; red, CellTracker Orange; blue, DAPI. Bars = 50 μm.

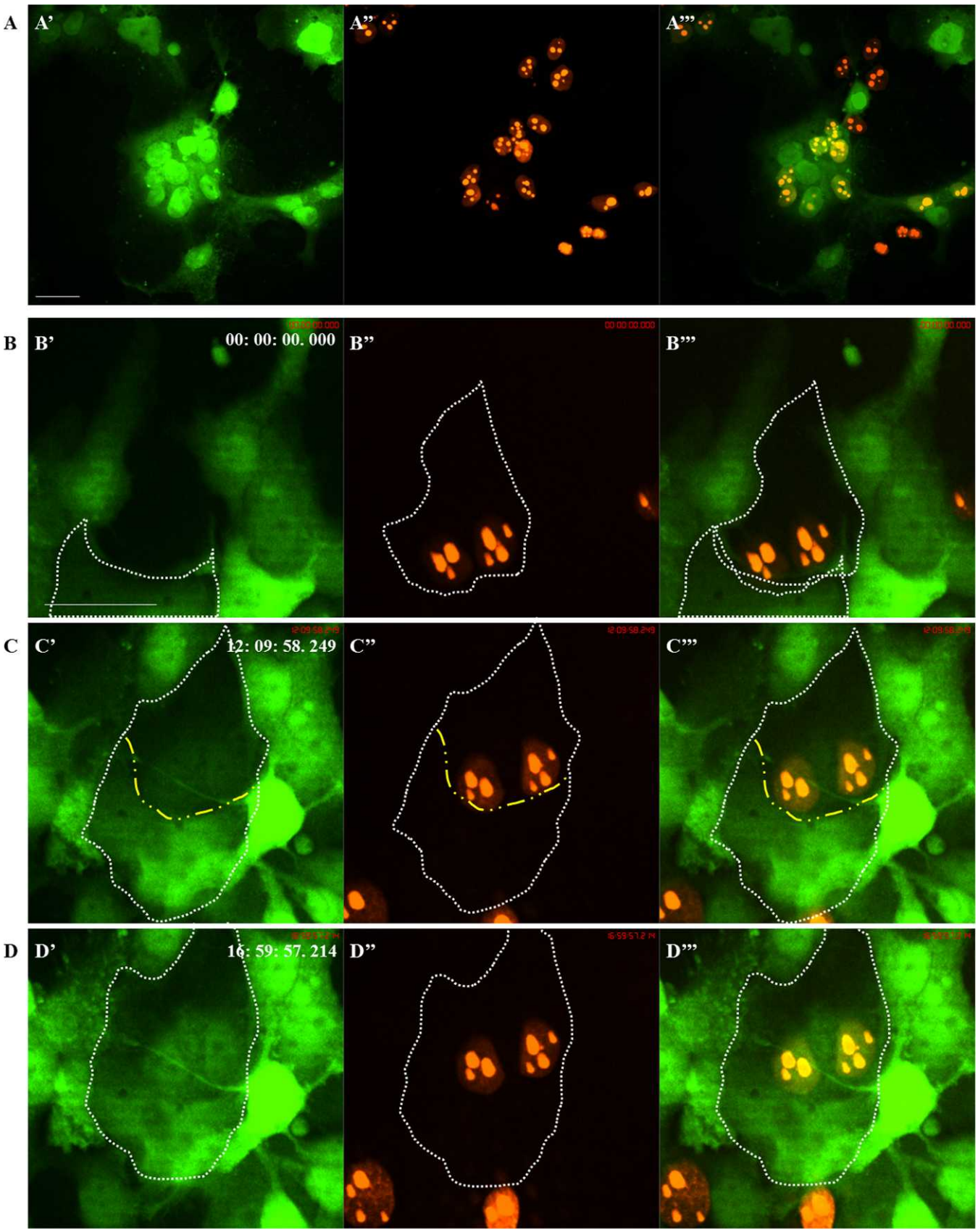

FIG. 4. Fluorescent live-cell imaging of BeWo cell-cell fusion using green and red fluorescent proteins as reporters. Still images from Supplemental Movie S5. BeWo cells were stably transfected with pEGFP-N1 or pDsRed2-Nuc reporter plasmids. The two stable cell lines were mixed in a 1:1 ratio and co-cultured with exposure to FSK for 48 h. **A**) BeWo cells stably expressing EGFP or nucleus-localized DsRed2-Nuc formed a multinucleated syncytium. **B**) Cells expressing EGFP ([**B**′] lower) and DsRed2-Nuc ([**B**″] upper) contacted each other (area inside dotted line). **C**) Green signals from the EGFP-expressing cell flowed gradually into the cytoplasm of the DsRed2-Nuc-expressing cell. The yellow dot-dash line shows the boundary between the fusing partners. **D**) After fusion, the syncytium was marked with both green cytoplasm and red nuclei. **A**‴, **B**‴, **C**‴, and **D**‴) Merged images. Bars = 50 μm. All experiments were repeated three times, and representative results are shown.

spontaneous fusion of primary CTBs and FSK-induced fusion of BeWo cells. Whether this exchange of cytoplasmic portions was asymmetrical and whether a similar fusion of the underlying cytotrophoblast layer toward the syncytiotrophoblast layer also occurs in vivo in human placentas needs to be characterized.

Time-lapse live-cell imaging studies, combined with electron microscopy and different molecular and genetic strategies, have been used to illustrate the dynamics of various cell fusion processes. For example, the complexity of hyphal growth and anastomosis in *Neurospora crassa* during fusion competence, contact, postcontact, and postfusion stages has been delineated. Morphologically different fusion-competent hyphae can sense ''fusion signals'' and redirect their growth, and cytoplasmic flow between the fusing hyphae occurs frequently [43]. Influenza hemagglutinin-induced cell fusion shows cytoplasmic continuity and lipid mixing with pH and temperature dependence [44]. During cell fusion in the embryonic epidermis of *C. elegans*, the initiation and completion of fusion are kinetically different, and the membrane from different sides of the same cell are distinct in their fusogenicity [24]. Furthermore, *eff-1* is required to control epidermal syncytiogenesis and expand the fusion pore [26–28], and *aff-1* is indispensable for anchor cell fusion, the fusion of two vulval rings [29]. F-actin foci at the site of *Drosophila* myoblast fusion have been recorded as transient structures, which appear and dissolve accompanying muscle growth [25]. Furthermore, the disrupted dynamics of actin polymerization have been observed in *blow* [45] and *dpak3* [46] mutant embryos. Recently, the actin regulator N-WASp was shown to be an essential contributor to myogenic cell-cell fusion in mice [47]. Based on the above observations, different developmental cell fusions have some common aspects (i.e., fusion-competent cells follow a well-ordered sequence to fuse), and different examples of cell fusion share some underlying mechanistic similarities.

Live-cell imaging using several color-based tools, such as the CellTracker cytoplasmic staining or constitutively expressing EGFP/DsRed2-Nuc in the present study, has shown for the first time the complexity of trophoblast cell-cell fusion. However, how trophoblast cell-cell fusion is precisely orchestrated by multifactorial networks remains to be further investigated. Are different trophoblast cell types (for example, fusion-competent cells and founder cells) present in trophoblast syncytialization? Does fusion pore expansion also occur in trophoblast cell-cell fusion? Do CTBs possess any polarity in their fusogenicity in vivo? How do syncytins and their related partners merge trophoblast membranes? The live-cell imaging systems that we have established and further optimized, such as shortening the image acquisition intervals, are undoubtedly powerful tools to address the above questions.

Based on the literature, the fusion index reported by different groups varies largely. In the present study, we therefore assessed the fusion indexes of both primary CTBs and FSK-treated BeWo cells by using both the CellTracker and E-cadherin staining methods and found a slight discrepancy between them. We believe that the fusion index discrepancy derived from the two quantification techniques is partially due to the fusion ability. For the cells with a higher ability to fuse, such as primary CTBs at later fusion stages, the discrepancy would be smaller than BeWo cells with lower fusion ability. Furthermore, both methods could omit the visualization of some multinucleated cells, in that (1) the fusion of cells with the same color was difficult to distinguish by CellTracker, and (2) some syncytium boundaries could not be clearly visualized by E-cadherin staining. Apart from the staining technique, more factors may contribute to variances in the fusion index; for example, the culture conditions and the concentration of FSK treatment of BeWo cells or the isolation method and the individual differences among donors of primary CTBs may affect the fusion index. In short, given the advantages and disadvantages of both techniques, they can reasonably be used together to quantify the fusion index.

In summary, we have provided valuable information for the dynamic process of trophoblast syncytium formation using live-cell microscopy. The live-cell imaging technique combined with multiple molecular biological strategies will provide a foundation for a new conceptual framework for understanding the cellular and structural mechanisms underlying human trophoblast syncytialization in vivo, which remains the least known process among all cell-cell fusion systems.

ACKNOWLEDGMENT

We thank Shi-Wen Li for technical assistance with confocal photography.

REFERENCES

1. Cross JC, Werb Z, Fisher SJ. Implantation and the placenta: key pieces of the development puzzle. Science 1994; 266:1508–1518.
2. Fu J, Lv X, Lin H, Wu L, Wang R, Zhou Z, Zhang B, Wang YL, Tsang BK, Zhu C, Wang H. Ubiquitin ligase cullin 7 induces epithelial-mesenchymal transition in human choriocarcinoma cells. J Biol Chem 2010; 285:10870–10879.
3. Potgens AJ, Schmitz U, Bose P, Versmold A, Kaufmann P, Frank HG. Mechanisms of syncytial fusion: a review. Placenta 2002; 23(suppl A): S107–113.
4. Huppertz B, Meiri H, Gizurarson S, Osol G, Sammar M. Placental protein 13 (PP13): a new biological target shifting individualized risk assessment to personalized drug design combating pre-eclampsia. Hum Reprod Update 2013; 19:391–405.
5. Rhodin JA, Terzakis J. The ultrastructure of the human full-term placenta. J Ultrastruct Res 1962; 6:88–106.
6. Terzakis JA. The ultrastructure of normal human first trimester placenta. J Ultrastruct Res 1963; 9:268–284.
7. Jones CJ, Fox H. Ultrastructure of the normal human placenta. Electron Microsc Rev 1991; 4:129–178.
8. Boyd JD, Hamilton WJ, Boyd CA. The surface of the syncytium of the human chorionic villus. J Anat 1968; 102:553–563.
9. Boyd JD, Hamilton WJ. Electron microscopic observations on the cytotrophoblast contribution to the syncytium in the human placenta. J Anat 1966; 100:535–548.
10. Huppertz B, Bartz C, Kokozidou M. Trophoblast fusion: fusogenic proteins, syncytins and ADAMs, and other prerequisites for syncytial fusion. Micron 2006; 37:509–517.
11. Pattillo RA, Gey GO, Delfs E, Mattingly RF. Human hormone production in vitro. Science 1968; 159:1467–1469.
12. Wice B, Menton D, Geuze H, Schwartz AL. Modulators of cyclic AMP metabolism induce syncytiotrophoblast formation in vitro. Exp Cell Res 1990; 186:306–316.
13. Kliman HJ, Nestler JE, Sermasi E, Sanger JM, Strauss JF, 3rd. Purification, characterization, and in vitro differentiation of cytotrophoblasts from human term placentae. Endocrinology 1986; 118:1567–1582.
14. Baczyk D, Dunk C, Huppertz B, Maxwell C, Reister F, Giannoulias D, Kingdom JC. Bi-potential behaviour of cytotrophoblasts in first trimester chorionic villi. Placenta 2006; 27:367–374.
15. Isaksen DE, Liu NJ, Weisblat DA. Inductive regulation of cell fusion in leech. Development 1999; 126:3381–3390.
16. Forest CL. Genetic control of plasma membrane adhesion and fusion in *Chlamydomonas* gametes. J Cell Sci 1987; 88(pt 5):613–621.
17. Glass NL, Rasmussen C, Roca MG, Read ND. Hyphal homing, fusion and mycelial interconnectedness. Trends Microbiol 2004; 12:135–141.
18. Podbilewicz B, White JG. Cell fusions in the developing epithelial of *C. elegans*. Dev Biol 1994; 161:408–424.
19. Chen EH. Invasive podosomes and myoblast fusion. Curr Top Membr 2011; 68:235–258.
20. Loutit JF, Nisbet NW. The origin of osteoclasts. Immunobiology 1982; 161:193–203.
21. Chambers TJ. Multinucleate giant cells. J Pathol 1978; 126:125–148.

22. Kahn AJ, Teitelbaum SL, Malone JD, Krukowski M. The relationship of monocytic cells to the differentiation and resorption of bone. Prog Clin Biol Res 1982; 110(pt B):239–248.
23. Vignery A. Osteoclasts and giant cells: macrophage-macrophage fusion mechanism. Int J Exp Pathol 2000; 81:291–304.
24. Gattegno T, Mittal A, Valansi C, Nguyen KC, Hall DH, Chernomordik LV, Podbilewicz B. Genetic control of fusion pore expansion in the epidermis of *Caenorhabditis elegans*. Mol Biol Cell 2007; 18:1153–1166.
25. Sens KL, Zhang S, Jin P, Duan R, Zhang G, Luo F, Parachini L, Chen EH. An invasive podosome-like structure promotes fusion pore formation during myoblast fusion. J Cell Biol 2010; 191:1013–1027.
26. Mohler WA, Shemer G, del Campo JJ, Valansi C, Opoku-Serebuoh E, Scranton V, Assaf N, White JG, Podbilewicz B. The type I membrane protein EFF-1 is essential for developmental cell fusion. Dev Cell 2002; 2: 355–362.
27. Podbilewicz B, Leikina E, Sapir A, Valansi C, Suissa M, Shemer G, Chernomordik LV. The C. elegans developmental fusogen EFF-1 mediates homotypic fusion in heterologous cells and in vivo. Dev Cell 2006; 11:471–481.
28. Oren-Suissa M, Hall DH, Treinin M, Shemer G, Podbilewicz B. The fusogen EFF-1 controls sculpting of mechanosensory dendrites. Science 2010; 328:1285–1288.
29. Sapir A, Choi J, Leikina E, Avinoam O, Valansi C, Chernomordik LV, Newman AP, Podbilewicz B. AFF-1, a FOS-1-regulated fusogen, mediates fusion of the anchor cell in *C. elegans*. Developmental Cell 2007; 12:683–698.
30. Borges M, Bose P, Frank HG, Kaufmann P, Potgens AJ. A two-colour fluorescence assay for the measurement of syncytial fusion between trophoblast-derived cell lines. Placenta 2003; 24:959–964.
31. Zhou Z, Zhang Q, Lu X, Wang R, Wang H, Wang YL, Zhu C, Lin HY, Wang H. The proprotein convertase furin is required for trophoblast syncytialization. Cell Death Dis 2013; 4:e593.
32. Guilbert LJ, Winkler-Lowen B, Sherburne R, Rote NS, Li H, Morrish DW. Preparation and functional characterization of villous cytotrophoblasts free of syncytial fragments. Placenta 2002; 23:175–183.
33. Lin FY, Chang CW, Cheong ML, Chen HC, Lee DY, Chang GD, Chen H. Dual-specificity phosphatase 23 mediates GCM1 dephosphorylation and activation. Nucleic Acids Res 2011; 39:848–861.
34. Redman CW, Sargent IL. Placental stress and pre-eclampsia: a revised view. Placenta 2009; 30(suppl A):S38–42.
35. Huppertz B. Placental origins of preeclampsia: challenging the current hypothesis. Hypertension 2008; 51:970–975.
36. Young BC, Levine RJ, Karumanchi SA. Pathogenesis of preeclampsia. Annu Rev Pathol 2010; 5:173–192.
37. Chen CP, Chen CY, Yang YC, Su TH, Chen H. Decreased placental GCM1 (glial cells missing) gene expression in pre-eclampsia. Placenta 2004; 25:413–421.
38. Chen CP, Wang KG, Chen CY, Yu C, Chuang HC, Chen H. Altered placental syncytin and its receptor ASCT2 expression in placental development and pre-eclampsia. BJOG 2006; 113:152–158.
39. Gauster M, Moser G, Orendi K, Huppertz B. Factors involved in regulating trophoblast fusion: potential role in the development of preeclampsia. Placenta 2009; 30(suppl A):S49–54.
40. Kesper DA, Stute C, Buttgereit D, Kreiskother N, Vishnu S, Fischbach KF, Renkawitz-Pohl R. Myoblast fusion in Drosophila melanogaster is mediated through a fusion-restricted myogenic-adhesive structure (FuRMAS). Dev Dyn 2007; 236:404–415.
41. Linder S, Wiesner C, Himmel M. Degrading devices: invadosomes in proteolytic cell invasion. Annu Rev Cell Dev Biol 2011; 27:185–211.
42. Lindau M, Almers W. Structure and function of fusion pores in exocytosis and ectoplasmic membrane fusion. Curr Opin Cell Biol 1995; 7:509–517.
43. Hickey PC, Jacobson D, Read ND, Glass NL. Live-cell imaging of vegetative hyphal fusion in *Neurospora crassa*. Fungal Genet Biol 2002; 37:109–119.
44. Sarkar DP, Morris SJ, Eidelman O, Zimmerberg J, Blumenthal R. Initial stages of influenza hemagglutinin-induced cell fusion monitored simultaneously by two fluorescent events: cytoplasmic continuity and lipid mixing. J Cell Biol 1989; 109:113–122.
45. Jin P, Duan R, Luo F, Zhang G, Hong SN, Chen EH. Competition between Blown fuse and WASP for WIP binding regulates the dynamics of WASP-dependent actin polymerization in vivo. Dev Cell 2011; 20: 623–638.
46. Duan R, Jin P, Luo F, Zhang G, Anderson N, Chen EH. Group I PAKs function downstream of Rac to promote podosome invasion during myoblast fusion in vivo. J Cell Biol 2012; 199:169–185.
47. Gruenbaum-Cohen Y, Harel I, Umansky KB, Tzahor E, Snapper SB, Shilo BZ, Schejter ED. The actin regulator N-WASp is required for muscle-cell fusion in mice. Proc Natl Acad Sci U S A 2012; 109:11211–11216.